CHAPTER XXX

SPATIAL MODELLING OF TRANSGENIC CONIFER POLLEN

GABRIEL KATUL[1,2], CLAIRE G. WILLIAMS[1], MARIO SIQUEIRA[1], DAVIDE POGGI [1,2,3], AMILCARE PORPORATO[2], HEATHER MCCARTHY[1], AND RAM OREN[1]

[1]*Nicholas School of the Environment and Earth Sciences, Box 90328, Duke University, Durham, NC 27708-0328, U.S.A.*

[2]*Department of Civil and Environmental Engineering, Duke University, Durham, NC 27708*

[3]*Dipartimento di Idraulica, Trasporti ed Infrastrutture Civili Politecnico di Torino, Torino, Italy.*

Abstract. Long-distance dispersal (LDD) of pollen in conifers presents a risk for transgenic escape into unmanaged forests. Here, we report simulations of transgenic pollen dispersal and LDD from genetically modified forests using a mechanistic turbulent dispersal model. The dispersal model is based on coupled Eulerian-Lagrangrian closure (CELC) principles that model turbulent velocity excursions within the canopy. Contrary to recent studies and measurements from annual crop canopies, which reported maximum pollen dispersal distances ranging from 6 m to 800 m, conifer pollen LDD can readily exceed 8 km in less than 1 hour without escaping the atmospheric boundary layer. These LDD estimates were conducted using a conservative terminal velocity (V_t) of 0.07 m s^{-1}. When using a V_t of 0.03 m s^{-1} $\pm$ 0.02 m s^{-1}, which is characteristic of pine species pollen, LDD increased by almost a factor of 3, from about 8 to 21 km for a stand at its reproductive onset and from about 13 km to 33 km for a stand at near-harvesting age. The fact that pollen can travel such distances without escaping the ABL has important consequences about viability and ecological risk assessment and gene flow.

INTRODUCTION

Estimating probability of transgenic pollen escape is timely because recombinant DNA technology to genetically modify forest trees is applied worldwide to commercially important species (Fenning and Gershenzon 2002), and pines are a

T.H.E. Editor(s) (ed.), Book title, 1 - 10.

major commodity species in both Northern and Southern Hemispheres. *Pinus taeda*, used here as a case study, is a long-lived woody perennial with delayed reproductive onset followed by abundant long-distance gene flow. *Pinus taeda* mating system is wind-pollinated and monoecious. Potential for transgenic escape is great because reproductive onset precedes harvest by a decade or more and there is natural hybridization and introgression among close relatives (Righter and Duffield 1951).

Few mechanistic models track long-distance dispersal (LDD) and escape probability of pollen from the canopy. However, several mechanistic models have been developed that predict attributes of seed and pollen dispersal kernels, such as means and modes (Okubo and Levin 1989, De Haan and Rotach 1998, Loos et al. 2003). LDD is often defined as the distance travelled by the 99% percentile of pollen (or seeds), though this definition is not be unique (Nathan et al. 2002, Cain et al. 2003, Higgins et al. 2003, Nathan et al. 2003). Most released pollen, however, will fall within the perimeter of the source, often referred to as local neighbourhood diffusion (LND) (Hengeveld 1989). Pollen dispersal can be viewed (and often modelled) as superposition of LND and LDD. Few stratified empirical diffusion models (Hengeveld 1989 pp. 48-53) even proposed bi-normal distribution kernels to account for these fundamentally different dispersion mechanisms (Nichols and Hewitt 1994, Bullock and Clarke 2000).

Pollen dispersal from conifer trees is different from that from agricultural crops in that tree height (h) accrues annually so released pollen is carried at increasing distances from a source, with a partial offset due to increased leaf area index (LAI) that attenuates mean wind speed and other turbulent statistics within the canopy. Windborne pollen LDD is associated with an uplifting process from within the canopy by turbulent eddies, comparable in size to h (Raupach et al. 1996, Katul et al. 1998, Poggi et al. 2004a, Poggi et al. 2004b) and then transported to elevated regions within the atmospheric boundary layer (ABL), and even higher into the troposphere, by larger-scale eddy motion. Given the large mean wind speeds at such elevations in the atmosphere, dispersal distances as far as 600 to 1200 km from the source can readily occur (Bessey 1883, Erdtman 1937, Lanner 1966, Di-Giovanni et al. 1995, Di-Giovanni et al. 1996). Even a simple ballistic model calculation suggests that at a settling velocity range of 25.3 to 31.9 mm s^{-1}, conifer pollen at 300 m above the surface moving at a speed of 5 ms^{-1} (assumed constant with height and time) would drift some 47 to 60 km in about 3 hours (Di-Giovanni et al. 1996). However, *P. taeda* pollen that has traveled for several hours or has escaped the ABL into the troposphere may not be viable because of the high exposure to UV-B radiation, and cold temperature (Tuskan et al. 1992). Most reports show that effective pollination distance of forest trees is more limited than recorded travel distances (Smouse et al. 2001). Similarly, studies on genetically modified (GM) corn pollen in Mexico found a slight viability loss after 1 hour of dispersion compared to a 100% viability loss after 2 hours of dispersion in wintertime (Aylor et al. 2003).

An immediate consequence of the above findings is that LDD might be less consequential than previously thought given the reduced pollen viability potential associated with its occurrence. Hence, quantifying the distances of pollen LDD for

events in which pollen did not escape from the top of the atmospheric boundary layer (~ 1 km high during daytime) or experienced long travel times (~ 1 hour) is central to ecological risk assessment. Yet, this combination of viability and distances are difficult to ascertain via field experiments.

To address this question, we adapt a three-dimensional coupled Eulerian-Lagrangian model (Hsieh et al. 2000, Nathan et al. 2002) to compute pollen dispersal kernels from a *P. taeda* plantation. Aylor and Flesch (2001) already used a simplified two-dimensional version of this model to compute spore concentrations of *Lycopodium* and *V. inaequalis* from a wheat canopy. The model parameters were estimated independently from meteorological, canopy and reproductive data collected at the Free Air CO_2 Enrichment (FACE) experiment at Duke University near Durham, North Carolina and used as a sample case study in the simulations.

METHODS

The CELC model calculations require the flow statistics above the canopy during the pollen release period along with the amounts and location of pollen released. *Pinus taeda* has male strobili within the lower 33% of the canopy so the release height was set at one-third the canopy height in all model calculations. Pollen release date was approximated using a heat sum model (Boyer 1978) for the Duke Forest plantation from 1999 to 2002 (Figure 1).

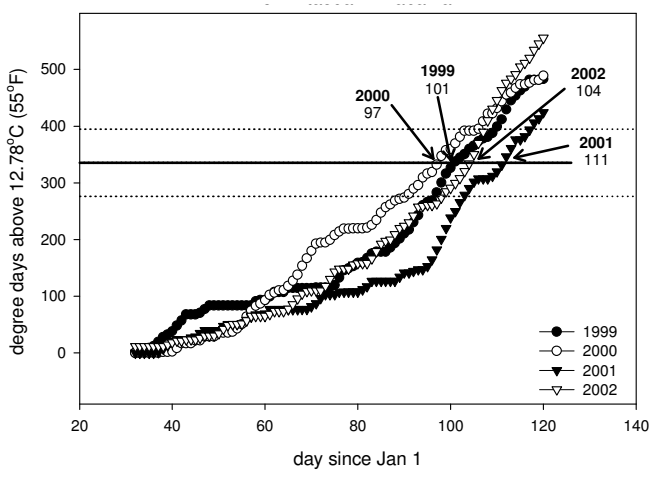

Figure 1: *Heat sum for pollen indicating Julian dates of production. Mean air temperature measurements collected at the Duke Forest FACE site are used.*

Based on the heat-sum model, pollen release occurs between April 1 and April 25. The concomitant velocity measurements needed by CELC are described later. Pollen dispersal quantity was based on pollen yield per tree per day. On average, one *P. taeda* tree at 16 m is estimated to produce 1133.9 grams of pollen over a 14-day pollen shed, roughly 81 g per tree per day on average (Parker and Blush 1996). Pollen grains (g^{-1}) usually range from 1.3 to 1.5 x 10^6. Hence, pollen production is about 113.4 x 10^6 pollen d^{-1} $tree^{-1}$. Using a tree density of a typical southern pine plantation (1750 trees ha^{-1}), the amount of pollen produced per 1 ha plantation is about $2x10^{11}$ pollen d^{-1}.

We used the long-term wind velocity data collected at the FACE facility, in Duke Forest (35º 97'N 79º 09' W) near Durham, North Carolina for driving the CELC model. The three velocity components and virtual potential temperature above the canopy were collected at 10 Hz using a CSAT3 (Campbell Scientific, Logan UT) triaxial sonic anemometer. These on-going velocity measurements commenced in 1998 and are part of a long-term CO_2 flux monitoring initiative (*Ameriflux*) within the United States (Baldocchi et al. 2001). The setup of the sonic anemometer, data collection, and post-processing are described elsewhere (Siqueira et al. 2000, Siqueira and Katul 2002, Siqueira et al. 2002). In addition, detailed leaf area density measurements collected during the pollen production period permit us to estimate how the flow statistics inside the canopy vary in relation to the measurements collected above the canopy (Katul and Albertson 1998, Katul and Chang 1999).

THEORY

After Thomson's seminal work (Thomson 1987), Lagrangian stochastic models for the trajectories of tracer-particles in turbulent flows are now routinely used in computational fluid mechanics and turbulence research (Pope 2000). These models are derived using the so-called well-mixed condition (*wmc*), which states that if a concentration of a scalar material is initially uniform at some time t_o it will remain so at any future time *t* in the absence of sources and sinks. The well-mixed condition is the most rigorous theoretical framework for computing Lagrangian trajectories and ensures consistency with prescribed Eulerian velocity statistics. Using the *wmc*, Thomson (1987) showed that the Lagrangian velocity of a tracer-particle is described by a generalized Langevin equation, of the form:

$$du_i = a_i(\vec{x},\vec{u},t)dt + b_{ij}(\vec{x},\vec{u},t)\,d\Omega_j$$

where $\vec{x}$ and $\vec{u}$ are the position and velocity vectors of a tracer-particle at time t, respectively. The terms a_i and b_{ij} are known as the drift and diffusion coefficients, respectively. The quantities $d\Omega_j$ are increments of a Wiener process with independent components, zero mean, and variance dt. Throughout, subscripts denote components of Cartesian tensors though both meteorological and index notations are also used interchangeably (i.e. the components of $\vec{x}$ are $x_1 = x$, $x_2 = y$, and

$x_3 = z$) with x, y, and z representing the longitudinal, lateral, and vertical axes, respectively. As discussed in Thomson (1987), b_{ij} can be uniquely determined by requiring that the Lagrangian velocity structure function in the so-called inertial sub-range match the well-known Kolmogorov's similarity theory (Rodean 1996). The determination of a_i remains a theoretical challenge requiring the use of *wmc*. For high Reynolds numbers, the *wmc* ensures that the Eulerian probability density function of the tracer particles $P(\vec{x},\vec{u},t)$ satisfies a Fokker-Planck equation,

$$\frac{\partial P}{\partial t}+\frac{\partial}{\partial x_i}(u_i P)=-\frac{\partial}{\partial u_i}(a_i P)+\frac{\partial^2}{\partial u_i \partial u_j}\left(\frac{1}{2}b_{ik}b_{jk}P\right).$$

The corresponding Langevin model of the above Fokker-Planck equation for a Gaussian, vertically inhomogeneous turbulence, consists of a set of three stochastic differential equations for the velocity components, given by (Thomson 1987):

$$du_1' = \left[-\frac{C_o<\varepsilon>}{2}(\lambda_{11}u_1'+\lambda_{13}u_3')+\frac{\partial<\bar{u}_1>}{\partial x_3}u_3'+\frac{1}{2}\frac{\partial<\overline{u_1'u_3'}>}{\partial x_3}\right]dt+\left[\frac{\partial<\overline{u_1'u_1'}>}{\partial x_3}(\lambda_{11}u_1'+\lambda_{13}u_3')+\frac{\partial<\overline{u_1'u_3'}>}{\partial x_3}u_1'+\lambda_{33}u_3'\right]\frac{u_3'}{2}dt+\sqrt{C_o<\varepsilon>}\;d\Omega$$

$$du_2' = \left[-\left(\frac{C_o<\varepsilon>}{2}+\frac{1}{2}\frac{\partial<\overline{u_2'u_2'}>}{\partial x_3}u_3'\right)(\lambda_{22}u_2')\right]dt+\sqrt{C_o<\varepsilon>}\;d\Omega$$

$$du_3' = \left[-\frac{C_o<\varepsilon>}{2}(\lambda_{13}u_1'+\lambda_{33}u_3')+\frac{1}{2}\frac{\partial<\overline{u_3'u_3'}>}{\partial x_3}\right]dt+\left[\frac{\partial<\overline{u_1'u_3'}>}{\partial x_3}(\lambda_{11}u_1'+\lambda_{13}u_3')+\frac{\partial<\overline{u_3'u_3'}>}{\partial x_3}(\lambda_{13}u_1'+\lambda_{33}u_3')\right]\frac{u_3'}{2}dt+\sqrt{C_o<\varepsilon>}\;d\Omega$$

where u_i' are the (instantaneous) turbulent velocities at position x_i and time t, C_0 (≈ 5.5) is a similarity constant (related to the Kolmogorov constant) and λ_{11}, λ_{13}, λ_{22}, and λ_{33} can be derived by inverting the Reynolds stress tensor, and are given by:

$$\lambda_{11} = \frac{1}{<\overline{u_1'u_1'}> - \frac{<\overline{u_1'u_3'}>^2}{<\overline{u_3'u_3'}>}}$$

$$\lambda_{22} = <\overline{u_2'u_2'}>^{-1}$$

$$\lambda_{33} = \frac{1}{<\overline{u_3'u_3'}> - \frac{<\overline{u_1'u_3'}>^2}{<\overline{u_1'u_1'}>}}$$

$$\lambda_{13} = \frac{1}{<\overline{u_1'u_3'}> - \frac{<\overline{u_1'u_1'}><\overline{u_3'u_3'}>}{<\overline{u_1'u_3'}>}}$$

Here, $<\overline{u_1}>$ is the mean longitudinal velocity (defined so that $<\overline{u_2}>=0$), $<\overline{u_1'u_1'}>(=\sigma_u^2)$, $<\overline{u_2'u_2'}>(=\sigma_v^2)$, $<\overline{u_3'u_3'}>(=\sigma_w^2)$, are the standard deviations of the three velocity components, $<\overline{u_1'u_3'}>$ (=$<\overline{w'u'}>$) is the Reynolds stress, and $<\bar{\varepsilon}>$ is the mean turbulent kinetic energy dissipation rate, < . > is spatial averaging (Raupach and Shaw 1982, Finnigan 2000), and over-bar is time averaging.

The vertical distribution of the flow statistics $<\overline{u_1}>$, $<\overline{u_1'u_1'}>$, $<\overline{u_2'u_2'}>$, $<\overline{u_3'u_3'}>$, $<\overline{u_1'u_3'}>$, and $<\bar{\varepsilon}>$ needed to drive the Thomson (1987) model can be readily computed from Eulerian second order closure models (Katul and Albertson 1998, Ayotte et al. 1999, Katul and Chang 1999, Massman and Weil 1999, Katul et al. 2001) as described in the Appendix. The above formulation, along with modeled $<\overline{u_1}>$, $<\overline{u_1'u_1'}>$, $<\overline{u_2'u_2'}>$, $<\overline{u_3'u_3'}>$, $<\overline{u_1'u_3'}>$, and $<\bar{\varepsilon}>$ using second order closure principles constitutes the formulation of the mean and turbulent velocity excursions within the CELC model (Nathan et al. 2002). With these velocity statistics, and for the purposes of estimating dt, we define the relaxation time scale by

$$T_L = \frac{0.5\times\left(\sigma_u^{\,2} + \sigma_v^{\,2} + \sigma_w^{\,2}\right)}{<\bar{\varepsilon}>}$$

and set $dt = 0.01T_L$ in all model calculations. This estimate of dt satisfies all the theoretical constraints discussed elsewhere (Reynolds 1998a, b, d, c). As stated

earlier, Aylor and Flesch (2001) used a 2-D version of the above model to estimate spore dispersion from a wheat canopy. Their model includes empirically specified profiles of $<\overline{u_1}>$, $<\overline{u_1'u_1'}>$, $<\overline{u_3'u_3'}>$, and $<\overline{u_1'u_3'}>$ and a simplified parameterisation for $<\overline{\varepsilon}>(=\frac{\sigma_w^{\ 2}}{C_o T_L}$, with T_L assumed constant inside the canopy, but for the particle trajectory equations, it was reduced to account for the inertia effects of heavy-particle when compared to the no-mass particle transport).

Recent experiments by Poggi et al. (2005) and theoretical arguments by Massman and Weil (1999) suggest that a constant length scale is more appropriate to modelling $<\overline{\varepsilon}>$ than a constant T_L. Also, a recent $K-\varepsilon$ study showed that either a constant length scale or the relaxation time scale (which varies inside the canopy) better describes the individual components of the mean turbulent kinetic energy dissipation rate budget (Katul et al. 2004). Notwithstanding these simplifications, the Aylor-Flesch comparisons between model calculations and measurements suggested that such class of Lagrangian dispersion models could realistically reproduce diaspore spread. We note here that the meteorological, terminal velocity, and leaf area density inputs to the CELC approach are identical to the Aylor-Flesch model (with the exception of the σ_v, which is required here). Loos et al. (2002) used a 1-D simplified analytical version of this model that is based on the localized near field (LNF) theory (Raupach 1983, 1987, Raupach 1989b, Raupach 1989a, Phillips et al. 1997, Siqueira et al. 2000) to successfully estimate the spread of GM pollen from transgenic maize. They also report good agreement between model calculations and measurements, at least within the 10 m from the source. However, the emphasis of the LNF method is based on a local homogenization of the near-field kernel so as to reproduce concentration variation neighbouring a source; the far-field kernel retains the usual gradient-diffusion approach. Hence, it is unlikely that LNF will be able to realistically simulate LDD for a canopy. Using an analytical approach, a solution for the dispersal kernel starting from a 3-dimensional Brownian motion for constant drift and dispersion coefficients from a point source can be derived (Stockmarr 2002). Stockmarr (2002) showed that upon radial averaging this solution, the power-law decay of the dispersal kernel tails is sensitive to whether a 2-D or a 3-D model is used. This perhaps motivates the retention of lateral dispersion in pollen dispersal calculations. Other approaches used to model LDD, such as the Puff model (Aylor et al. 2003), lack the detailed description of canopy turbulence needed to ensure realistic escape probabilities from the canopy. The simulations proposed here are among the most detailed three-dimensional simulations for pollen release inside a southern pine forest and consider the effect of age, through its effect on tree height, on *P. taeda* pollen dispersal kernels. We emphasize that the same approach can be used for calculating LDD of seeds (e.g., Nathan et al. 2002).

MODEL SIMULATIONS

The pollen simulations were performed for the *P. taeda* plantation at reproductive onset (16 years; 14.6 m tall), and at a typical harvest age (25 years; 21.3 m tall).

Table 1: CELC model input and output variables for *P. taeda* pollen dispersal using measured meteorological and stand characteristics. The pollen release height, canopy height, and the normalized mean wind speed at the release height are also shown. The statistics pertaining to the dispersal kernels in Figures 4 and 5 are also presented. These statistics include the mode, the mean distance of the furthest 1% pollen ($D_{99\%}$), the fraction of pollen that travelled more than1 km, the probability that pollen escapes the canopy volume, and the mean travel time corresponding to the pollen particle (D_{99}) are presented for the two age classes. The dispersal calculations are shown for mean terminal velocities of 0.03 ± 0.02 and 0.07 ± 0.02.

Variables	*Dispersal Statistics*			
	16 years		*25 years*	
Release Height (m)	*4.87*		*7.1*	
Canopy Height (m)	*14.6*		*21.3*	
LAI (m^2 m^{-2})	*2.3*		*3.1*	
U / u_* (at $h/3$)	*1.14*		*0.78*	
u_* for dislodging (m s^{-1})	*0.44*		*0.64*	
Terminal Velocity (m s^{-1})	*0.07*	*0.03*	*0.07*	*0.03*
Mode (km)	*0.31*	*1.58*	*0.41*	*2.47*
$D_{99\%}$ (km)	*8.62*	*21.0*	*13.5*	*33.5*
Fraction of pollen > 1 km (%)	*4.3*	*24.9*	*4.8*	*28.2*
Probability of escape from the canopy volume (%)	*6.4*	*27.5*	*4.4*	*24.3*
Travel Time of D_{99} (h)	*0.35*	*0.73*	*0.51*	*0.81*
D_{max} (km)	*26.8*	*49.6*	*43.6*	*60.0*

The release height and leaf area index (LAI) for these two age classes are presented in Table 1. The estimates of canopy height and LAI for the March-April period are for the moderately low fertility site of the Duke Forest (Oren et al. 2001).

The model computes the trajectory of a pollen particle with time from the release height until it is absorbed at the ground for a given u_* ($=\sqrt{-\overline{u_1' u_3'}}$), the friction velocity above the canopy. Pollen particles that reach 1 km elevation or travel the flow domain for more than 1 hour are considered unviable (or dead) and excluded. The model releases pollen when the local mean wind speed ($<\overline{u_1}>$) at the release height (see Table 1) exceeds 0.5 m s^{-1} (Aylor and Parlange 1975). This velocity was defined as a minimum velocity necessary to dislodge pollen by minor leaf fluttering or ventilation. Similarly, Aylor et al. (2003) found that corn pollen dislodges at a $<\overline{u_1}>$ between 0.25 and 0.5 m s^{-1}. This threshold necessitates that u_* above the canopy must exceed a certain rate before pollen release occurs, which can vary among the two age classes considered here (see Table 1). To extrapolate the mean wind conditions for "extreme" scenarios not recorded within the 5-year velocity record at the site, the 30-minute 5-year sonic anemometer measured u_* distribution collected was fitted to a Weibull function. The Weibull probability density function (pdf) for u_* is given

$$pdf(u_*) = \frac{c\,{u_*}^{c-1}}{b^c} \exp\left(-\left[\frac{u_*}{b}\right]^c\right)$$

Here, b and c are shape and scale parameters, respectively, and can be determined from the sonic-anemometer measured u_* using the Method of Maximum Likelihood (MML). Using the MML, b and c can be determined by solving the two nonlinear equations:

$$b = \left[\frac{1}{n}\sum_{i=1}^{n}\left[u_*(i)\right]^c\right]$$

$$c = \frac{n}{\left(\frac{1}{b}\right)^c \sum_{i=1}^{n}\left[u_*(i)\right]^c \log(u_*(i)) - \sum_{i=1}^{n}\log(u_*(i))}$$

where $u_*(i)$ (i = 1, 2, …n) are the sonic anemometer measured u_* time series, and n (= 39,273) is the number of u_* measurements used in the estimation of b (=0.456)

and c(=2.11) as shown in Figure 2. To insure fully-developed turbulence conditions inside the canopy, all $u_*(i) < 0.1$ m s^{-1} were excluded from the b and c calculations (Lai et al., 2002). Furthermore, these small u_* do not contribute to pollen dislodging. As evidenced from Figure 2, the agreement between the Weibull function and the measured $pdf(u_*)$ is reasonably well for $u_*(i) >$ 0.1 m s^{-1}, especially at the measured tails.

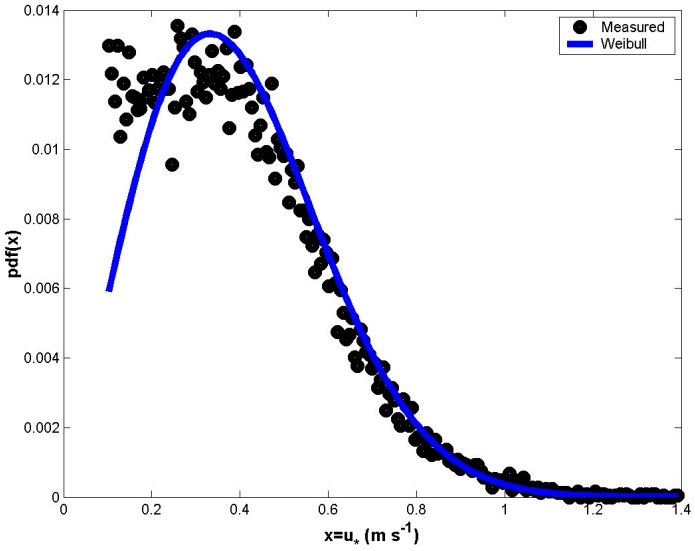

***Figure 2**: Measured and modelled probability distribution functions (pdf) of sonic anemometer measured friction velocity (u_*) above the pine canopy (1998-2003). The Weibull parameters are b =0.456 and c=2.11 as determined from MML.*

It is desirable to use the widest possible range in u_* variability for estimating the parameters of the Weibull function; however, it is not clear whether this distribution is "representative" of the wind conditions during the pollination period shown in Figure 1. Hence, we conducted a Kolmogorov-Smirnov test (Press et al. 1992) to assess whether the histogram of the entire u_* record (divided into 30 bins) is consistent with the u_* distribution for the March-April months from 1998-2003. We found that the two distributions were not statistically different at the 95% confidence level and the Weibull parameters obtained from the entire record of

$u_*(i)$ statistically represent the wind conditions during the pollination months. The pollen particle trajectories were computed as follows:

(i) Using the leaf area density and index (see Table 1), the Eulerian second-order closure model in the Appendix is used to compute the normalized $<\overline{u_1}>$, $<\overline{u_1'u_1'}>$, $<\overline{u_2'u_2'}>$, $<\overline{u_3'u_3'}>$, $<\overline{u_1'u_3'}>$, and $<\overline{\varepsilon}>$. The normalizing variables in the second-order closure model are u_* above the canopy and h.

(ii) A random u_* from the Weibull distribution was selected using

$$u_* = b\left(\log\left[\frac{1}{1-\mu}\right]\right)^{1/c}$$

where $\mu \in [0,1]$ is a uniform deviate random number, generated using the algorithm in Press et al. (1992). If u_* does not exceed the threshold u_* necessary to generate a $<\overline{u_1}> > 0.5$ m s^{-1} at the release height (see Table 1), no pollen particle is released and a new u_* is generated. Note that the maximum u_* generated from this approach can exceed the maximum recorded u_* within the 5-year record.

(iii) Using the generated u_*, h, and the normalized flow statistics from step (i), $<\overline{u_1}>$, $<\overline{u_1'u_1'}>$, $<\overline{u_2'u_2'}>$, $<\overline{u_3'u_3'}>$, $<\overline{u_1'u_3'}>$, and $<\overline{\varepsilon}>$ along with their vertical gradients are computed.

(iv) The three stochastic differential equations are simultaneously solved using the inputs from step (iii) for the turbulent velocity excursions along with the trajectory equation

$$x_i(t+dt) = x_i(t) + \int_t^{t+dt} \left(<\overline{u_i}>\delta_{i1} - V_t\delta_{i3} + u_i'\right)dt$$

where δ_{ij} is the Kronecker delta tensor, and V_t is the pollen terminal velocity. The estimation of V_t and dt are considered next. Di-Giovanni et al. (1995) reported a mean V_t for black spruce (*Picea mariana*) of 0.0319 m s^{-1} and for jack pine (*Pinus banksiana*) of 0.0253 m s^{-1}. They did not find any statistical difference in

V_t between clustered and un-clustered pollen for these two species (Di-Giovanni et al. 1995). Notwithstanding statistical significance, their V_t measurement for black spruce and for triple grains (clumped) is 0.0626 ± 0.013 m s^{-1}. This estimate, which is an upper limit for conifer V_t, motivated us to choose a conservative V_t of 0.07 ± 0.02 ms^{-1} in the model calculations. Formal sensitivity analysis on V_t will be described in our discussions later.

Regarding the estimates of dt from T_L, it has been argued that a heavy particle has a smaller time scale T_L when compared to a weightless (or passive) particle (Sawford and Guest 1991, Wilson and Sawford 1996, Reynolds 2000, Reynolds and Cohen 2002). Sawford and Guest (1991) estimate that the difference between the passive and heavy particle time scale is given by

$$T_L^{\,heavy\ particle} = \frac{T_L^{\,passive\ partlice}}{\sqrt{1+\beta'\left(\frac{V_t}{\sigma_w}\right)^2}}$$

where β' relates the Lagrangian and Eulerian time scales. The β' ranges from 1.0 to 1.5 (Raupach 1989a, c). With a conservative estimate of $\beta' \approx 1.5$, and noting that 1) $\sigma_w \sim u_*$ near the canopy top, 2) a minimum $u_* = 0.44$ m s^{-1} is needed to dislodge pollen from the bottom third of the canopy, the time scale correction (with $V_t = 0.07$ m s^{-1}) is about 1.019 or 1.9%. Hence, to a first order, coniferous pollen can be treated as a passive particle for the purposes of time scale calculations. The pollen release is initiated from rest ($u_i = 0$) at the release height ($= h/3$) from the ground. The radial distance from the source, the maximum elevation, and the travel time duration are recorded when the pollen particle arrives at the forest floor, assumed to be an absorbing boundary condition. An absorbing boundary condition prohibits re-suspension of the pollen into the air after falling on the ground. These trajectory calculations do not consider many other factors such as adsorption (and re-suspension) of pollen on canopy elements, or the effect of heavy rain that produce pollen washout from the air (Aylor and Flesch 2001). This latter point will also be discussed within the context of the measured precipitation at the site.

RESULTS

As described earlier, the simulations for the reproductive and near-harvesting stages primarily differ in LAI and pollen release height. Difference in LAI between the early reproductive age (2.3 m^2 m^{-2}) and near-harvesting age (3.2 m^2 m^{-2}) of *P. taeda* is sufficiently large to impact the flow statistics inside the canopy (Figure 3). It is

clear from Figure 3 that a 30% increase in LAI impacts primarily the second-order turbulence statistics (e.g. $<\overline{u_1' u_1'}>$, $<\overline{u_3' u_3'}>$, and $<\overline{u_1' u_3'}>$) and not as much $<\overline{u_1}>$.

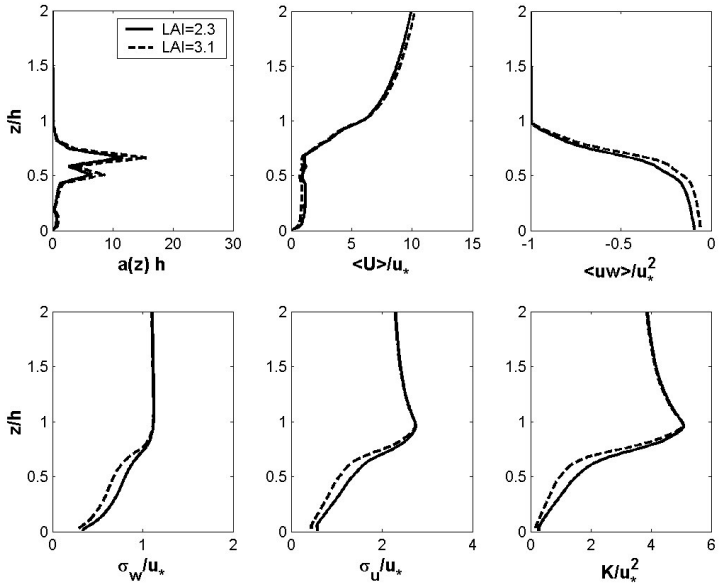

***Figure 3**: Modelled velocity statistics profiles needed to drive CELC model for the 16-year old (solid) and 25 year old (dashed) plantations. The normalized leaf area density is also shown.*

Whether the increased attenuation of the second-order flow statistics with increasing LAI can be compensated for by increase in pollen release height will be considered. The dispersal kernels for the reproductive onset age and the typical harvest age were compared in Figure 4a. The key statistical attributes of these kernels are summarized in Table 1. Both modelled kernels suggest that pollen LDD are in excess of 8 km, and can be achieved without pollen escaping from the ABL. The mean travel time, corresponding to D_{99}, does not exceed one hour for all particles reported in Figures 4a (and 4b). While the increase in LAI at harvest age dampens the turbulence statistics within the canopy (see Figure 3), the increase in pollen release height more than compensates - resulting in a greater mode and larger LDD (Table 1). Regarding the escape probabilities ($\Pr(z > h)$) from the canopy volume, the results in Table 1 appear counter-intuitive. We expected that for the 25-year old stand, $\Pr(z > h)$ would be larger than the 16-year old stand because of a longer settling (or

residence) time within the canopy, and hence, higher probability of encountering an ejection event. However, although the turbulent kinetic energy is about the same within the region $h/3$ and h in both stands, the smaller $<\bar{\varepsilon}>$ in the younger stand makes the flow appear more organized (i.e large T_L).

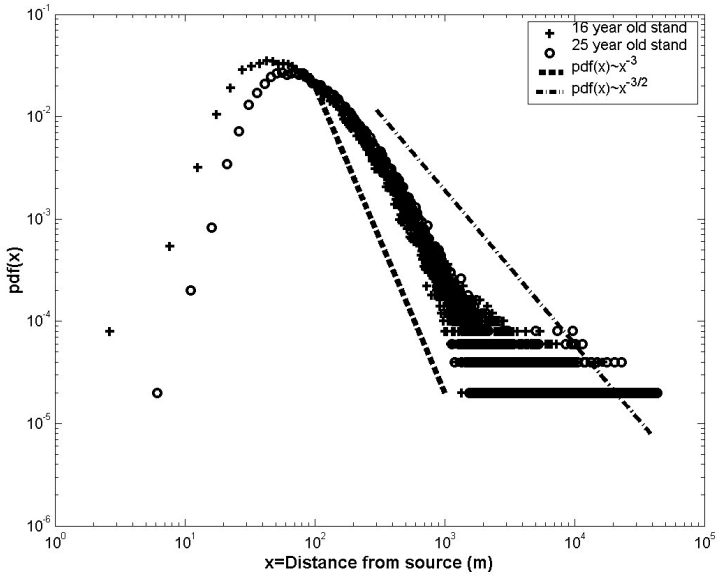

Figure 4a: Modelled dispersal kernels for the 16 year old and 25 year old P. taeda stands using 10^6 particles per age class. The –3 and –3/2 power-law decay of the dispersal kernels are shown for reference.

More organized flow leads to more coherent upward vertical motion, and hence, greater escape probability. Thus, while the pollen in the 25-year old-stand has a higher probability of encountering an updraft because of the longer residence time inside the canopy volume, its upward trajectory is less coherent when compared to the pollen trajectories in the 16-year old stand. The kernels in Figure 4a also exhibit approximate power-law decay between 200 m and 800 m. The power-law decay rate within this range has an approximate exponent = –3, which is steeper than the -1.78 reported by Aylor et al. (2003) for corn pollen (that was bounded between 10 m and 60 m). As discussed in Aylor et al. (2003), power-law tails suggest fat-tailed distributions. Interestingly, Figure 4a also suggests that beyond 1 km, the kernels clearly exhibit fat-tails that decay slower than –1.5. Kernel tails might exhibit different behaviour beyond 1 km due to pollen escape from the canopy volume encountering a turbulent flow field with different statistical properties than

the flow inside the canopy. The flow above the canopy resembles a rough-wall boundary layer and has a larger integral time scale (i.e. also more coherent), a larger σ_w and $\bar{u}$. To illustrate this point further, we recomputed the kernels in Figure 4a after removing all distances associated with pollen that escaped from the canopy (Figure 4b). It is clear from this figure that much of the dispersal events that yielded distances > 3 km can be attributed to pollen escaping the canopy volume.

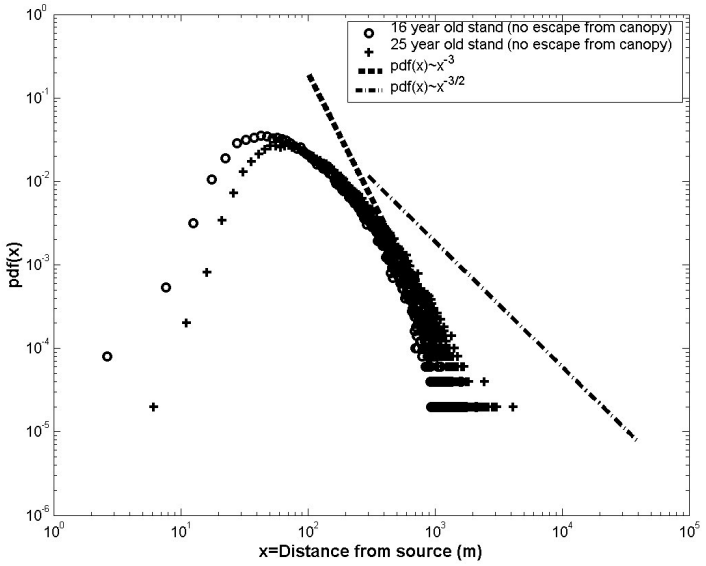

Figure 4b: Same as Figure 4a but excluding pollen that escaped the canopy volume.

To assess how sensitive the results in Table 1 are to the assumed V_t, we repeated all the calculations in Figure 4 for a V_t consistent with the mean (single-grained) V_t for black spruce and jack pine. This V_t is about 80% smaller than the V_t value used in Figure 4 (0.03 ± 0.02 m s^{-1} versus 0.07 ± 0.02 m s^{-1}). We found that the overall dispersal statistics in Table 1 are sensitive to V_t. Not surprisingly, the mode, LDD, and fraction of pollen escaping the canopy all increased with decreasing V_t. In fact, LDD increased nearly 3-fold for such an increase in V_t. Even the exponent of the power-law decay (see Figure 5a) has shifted closer to –1.5 for the reduced V_t, consistent with Stockmarr (2002) solution for "zero gravity". Simulations with

$V_t \to 0$ are analogous to simulations in zero gravity. Again, for this reduced V_t, we find that the heavy-tails can be attributed to the pollen escape from the canopy volume as evidenced by Figure 5b.

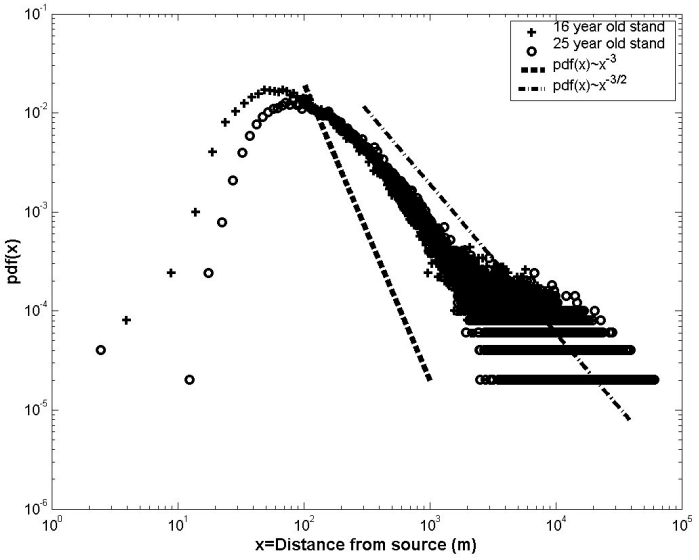

***Figure 5a**: Same as Figure 4a but for $V_t = 0.03 \pm 0.02$ m s^{-1}.*

As mentioned, rainfall intensity (R_I) can impact pollen trajectories by removing or washing pollen from the air. Aylor and Flesch (2001) found, for example, that a rainfall rate of 10 mm h^{-1} is too small for any washout to occur for *Venturia inaequalis* pollen. However, for larger intensities, they found that the loss of pollen from the air varies as $R_I^{0.787}$. Using the 30 minute-precipitation measurements collected at the site from 1998-2003 along with their threshold for washout, less than 10% of the 30-minute runs have rainfall events exceeding 0.1 mm h^{-1} (includes day and night), and we also found that 95% of the rainfall events have precipitation intensity not exceeding 10 mm h^{-1} (Figure 6). Hence, it is likely that for this site washout will not play a first-order effect on LDD in this southeastern pine forest.

We note that the calculations leading to the summary results in Table 1 and Figures 4 and 5 neglect key processes known to affect pollen dispersal such as 1) pollen deposition and re-suspension on vegetation organs, 2) re-suspension from the forest floor, and 3) pollen washout from vegetated surface by rain. These processes tend to reduce pollen viability because of the increase in transport time. Hence, in a first

order analysis, the distances reported in Table 1 are likely to serve as an upper limit on LDD for the wind statistics shown in Figure 2. Nonetheless, such upper limits are needed when gene flow and concomitant ecological risk assessments are being evaluated.

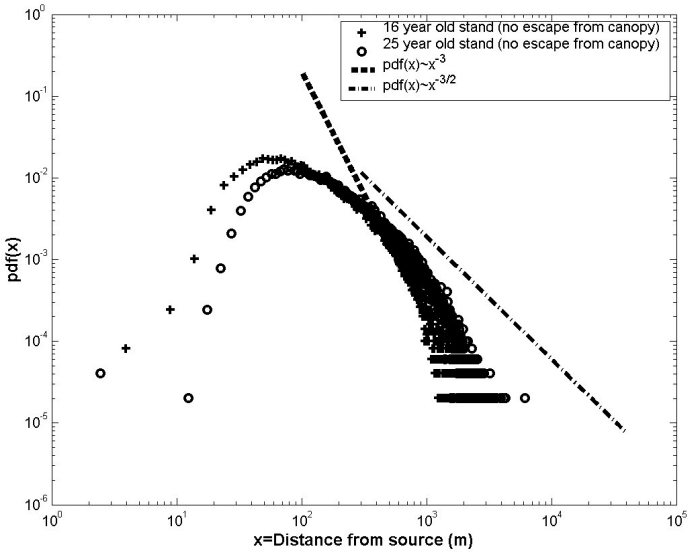

***Figure 5b**: Same as Figure 4b but for* $V_t = 0.03 \pm 0.02$ *m s*$^{-1}$.

DISCUSSION AND CONCLUSIONS

Globally, public concern about risks associated with GM releases in geographic areas populated with diverse plants is proliferating exponentially (e.g. Hails, 2000; Strauss et al., 2001; Mann and Plumer, 2002). It was proposed that gene flow be managed using physical isolation distances, often determined from empirical farm scale experiments or subjective risk assessments relying on expert opinions (e.g. OGTR, 2001; Gura, 2001). For GM agricultural crops, we note that expert opinions may not be subjective because studies of gene flow for GM pollen in the past decade are numerous, in sharp contrast to studies of transgenic pollen of forest tree species. For example, pollen dispersal studies for maize *(Zea mays* L.) suggest a 7.5 –30 m maximum distance (Jarosz et al. 2003, Loos et al. 2003).

***Table 2**: Recommended isolation distances for several GM crops (see review by Messeguer, 2003) and/or maximum distance from the source in which pollen grains were detected.*

Crop	***Comments***	***Reference***
	Crops	
Oilseed rape	*Frequency of hybrid formation (GM and non-GM) was 0.156% at 200 m and 0.0038% at 400 m.*	*Messeguer (2003)*
Maize (corn*)* *(Zea mays* L.*)*	*Most pollen fell within 5 m, 98% of the pollen remained within a 25–50 m.*	*Same*
Cultivated rice (*Oryza sativa* L.*)*	*Pollen horizontal movement was limited to 10 m.*	*Same*
Potato *(Solanum tuberosum* L.*)*	*Isolation distance of 20 m appears adequate for transgenic potatoes. However, maximum distances for which pollen particles were detected is 80 m.*	*Messeguer (2003) & Moyes and Dale (1999).*
Cotton *(Gossypium hirustum* L.*)*	*Pollen trapped decrease to 0.03% at 50 m from the source. Other studies concluded that isolation distances of 50 m from the source are adequate.*	*Messeguer (2003)*
Wheat	*Maximum distance pollen were detected is 20 m*	*Same*
	Trees	
Apples	*Maximum distance pollen particles were detected is 56 m*	*(Moyes et al. 2002)*
Eucalypt Forest	*Minimum modelled distance to minimize gene flow between GM and wild forest stands is >> 100 m*	*Lincare and Ades (2004)*
Pinus taeda	*LDD ranges from 26 - 60 km. Distances are for pollen particles that travelled < 1 hour and remained within the atmospheric boundary layer.*	*This study*

Pollen experiments for canola (*Brassica rapa*) found viable pollen at distances greater than 1 km (Rieger et al. 2002, Messeguer 2003). Isolation distances for several annual GM crops are summarized in Table 2 along with estimates of the maximum distances for transgenic pollen (Christey and Woodfield 2001). Our model results show that transgenic conifer pollen is likely to disperse at least 2 orders of magnitude more than GM crops. Hence, an isolation distance based on the minimum limit established for seed production (i.e. 0.1% of pollen arriving at a location) would lead to bio-containment or isolation zones for *P. taeda* well in excess of 1 km. These model results are consistent with modelled gene flow results for *Eucalyptus* plantation, obtained from recent cellular automaton calculations that included both pollen and seed dispersal, mortality effects, disturbances, and fecundity (Lincare and Ades, 2004).

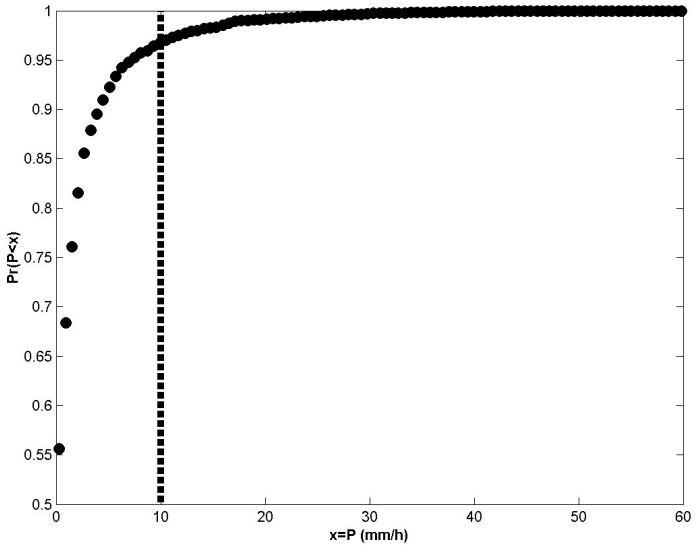

Figure 6: Cumulative precipitation (P) probability distribution function (Pr) for P>0. More than 95% of the precipitation events have intensities not exceeding 10 mm h-1 (vertical line).

Furthermore, our simulations suggest that conifer pollen is not likely to be of negligible viability at those distances due to excess UV-B, cold air temperatures, or dehydration, because of the short time interval for such long-distance movement. Given the long dispersal distances reported here, a regulatory framework that distinguishes between perennial crops and forests is only logical and has been advocated for almost a decade (e.g. Strauss et al., 1995). Lincare and Ades (2004) stated that "*a less subjective and more transparent method is required for the proper*

evaluation of risk reduction measures" if the general public is to accept the use of GM trees. Here, we show that stochastic models of particle dispersion in turbulent flows can augment risk assessments because model assumptions are explicit (*or transparent*) and the capacity to simulate ensemble of "worst-case" scenarios for a wide range of parameter space (*or proper evaluation of risk*) are now computationally possible.

ACKNOWLEDGEMENTS

Katul, Williams, and Oren acknowledge support from the Center on Global Change at Duke University. This project was supported by the US National Science Foundation (NSF-EAR), the Biological and Environmental Research, (BER) Program, U.S. Department of Energy, through the Southeast Regional Center (SERC) of the National Institute for Global Environmental Change (NIGEC), and through the Terrestrial Carbon Processes Program (TCP) and the FACE project.

APPENDIX: SECOND-ORDER CLOSURE MODEL FOR THE EULERIAN FLOW STATISTICS

In this appendix, the estimation of the Eulerian flow statistics needed to drive the Thomson (1987) Lagrangian dispersion model are described, followed by the numerical scheme, closure constants, and boundary conditions. Upon temporal and spatial averaging the conservation of momentum equations, and following the closure approximations of canopy flows (Wilson and Shaw 1977), the standard second order closure model of Wilson and Shaw simplifies to the following set of ordinary differential equations (ODEs):

Mean Momentum:

$$0 = -\frac{d<\overline{u'w'}>}{dz} - C_d\, a(z) <\bar{u}>^2$$

Tangential Stress Budget:

$$0 = -<\overline{w'^2}>\frac{d<\bar{u}>}{dz} + 2\frac{d}{dz}\left(q\lambda_1 \frac{d<\overline{u'w'}>}{dz}\right) - \frac{q<\overline{u'w'}>}{3\lambda_2} + C\,q^2\frac{d<\bar{u}>}{dz}$$

Longitudinal Velocity Variance:

$$0 = -2 < \overline{u' w'} > \frac{d < \bar{u} >}{d z} + \frac{d}{d z}\left(q \lambda_1 \frac{d < \overline{u'^2} >}{d z} \right) + 2 C_d a(z) < \bar{u} >^3 - \frac{q}{3 \lambda_2}\left(< \overline{u'^2} > - \frac{q^2}{3} \right) - \frac{2}{3}\frac{q^3}{\lambda_3}$$

Lateral Velocity Variance:

$$0 = \frac{d}{d z}\left(q \lambda_1 \frac{d < \overline{v'^2} >}{d z} \right) - \frac{q}{3 \lambda_2}\left(< \overline{v'^2} > - \frac{q^2}{3} \right) - \frac{2}{3}\frac{q^3}{\lambda_3}$$

Vertical Velocity Variance:

$$0 = \frac{d}{d z}\left(3q \lambda_1 \frac{d < \overline{w'^2} >}{d z} \right) - \frac{q}{3 \lambda_2}\left(< \overline{w'^2} > - \frac{q^2}{3} \right) - \frac{2}{3}\frac{q^3}{\lambda_3}$$

Where $q = \sqrt{< \overline{u_i' u_i'} >}$ is a characteristic velocity scale, C_d is a drag coefficient, $a(z)$ is a leaf area density, $\lambda_j = a_j L_{ws}$, with L_{ws} a characteristic length scale specified using the formulation in Katul and Albertson (1998) and is not permitted to increase at a rate larger than k, the Von Karman constant, and a_1, a_2, a_3 and C are determined so that the flow conditions well above the canopy reproduce well-established surface layer similarity relations. With estimates of the five constants (a_1, a_2, a_3, C, and α), the above five ODEs can be solved iteratively for the five flow variables $< \bar{u} >, < \overline{u'w'} >$, $< \overline{u'^2} >$, $< \overline{v'^2} >$, $< \overline{w'^2} >$, which are used to drive the Lagrangian model. Note that this approach neglects dispersive fluxes, which appears to be reasonable for dense canopies (Poggi et al., 2005).

A.1 The Computational Grid

The computational flow domain was set from zero to 50×h. The grid node spacing is Δz = 0.05 m. This grid density was necessary due to rapid variability in leaf area density close to the canopy top. Parameter values at the exact location of the pollen are calculated by interpolation between the grid nodes.

A.2 The Numerical Scheme

The five ODEs for the Wilson and Shaw (1977) model were first discretized by central differencing all derivatives. An implicit numerical scheme was constructed for each ODE with boundary conditions to be discussed in section *A.3*. The tridiagonal system resulting from the implicit forms of each discretized equation was solved using the *Tridag* routine in Press et al. (1992, pp.42-43) to produce the turbulent statistic profile. Profiles for all variables were initially assumed, and a relaxation scheme was used for all computed variables (Wilson 1988). Relaxation factors as small as 5% were necessary in the iterative scheme because of the irregularity in the leaf area density profile. The measured leaf area density was interpolated at the computational grid nodes by a cubic-spline to insure finite second derivatives of $a(z)$. Convergence is achieved when the maximum difference between two successive iterations in $<\bar{u}>$ did not exceed 0.0001%. We checked that all solutions were independent of Δz.

A.3 Boundary Conditions and Closure Constants

Typically, the well-established flow statistics in the atmospheric surface layer provide convenient upper-boundary conditions for closure models. The boundary conditions used are:

$$z = 0 \qquad \begin{cases} \sigma_u = & 0 \\ \sigma_v = & 0 \\ \sigma_w = & 0 \\ u_* = & 0 \\ <\bar{u}> = & 0 \end{cases}$$

$$z = 50 \times h \qquad \begin{cases} \sigma_u = & A_u u_* \\ \sigma_v = & A_v u_* \\ \sigma_w = & A_w u_* \\ u_* = & 1 \\ \dfrac{d<\bar{u}>}{dz} = & \dfrac{u_*}{k_v(z-d)} \end{cases}$$

Where σ_θ is the standard deviation of any flow variable $\theta (=<\theta'^2>^{1/2})$, A_u=2.2, A_v=2.0, and A_w=1.4 (Katul and Chang, 1999). The closure constants are dependent on the choice of the boundary conditions and are determined by assuming that in the atmospheric surface layer ($z > 2h$), the flux-transport term is negligible and that $<\overline{u'w'}>, <\overline{u'^2}>^{1/2}$, and $<\overline{w'^2}>^{1/2}$ become independent of z for near-neutral

conditions. These simplifications result, after some algebraic manipulations, in the following relationships between A_u, A_v, and A_w and a_2, a_3, and C:

$$a_2 = \frac{A_q(A_u^2 - A_w^2)}{6}$$

$$a_3 = \frac{-A_q^3(A_u^2 - A_w^2)}{A_w^2 - \frac{A_q^2}{3}}$$

$$C = \left(\frac{A_w}{A_q}\right)^2 - \frac{2}{A_q^2(A_u^2 - A_w^2)}$$

Where $A_q=(A_u^2+A_v^2+A_w^2)^{1/2}$. The closure constant a_1 is determined by noting that the "eddy-diffusivity" is $k(z-d)u_*$ in the surface layer. Hence, $q\lambda_1$ becomes identical to $k(z-d)u_*$ leading to $a_1=1/A_q$. The above equations are the first analytic expressions relating closure constants to ASL boundary conditions for the Wilson and Shaw (1977) model. Table A1 summarizes the closure constants used resulting from our choice of A_u, A_v, and A_w.

Table A1. *Closure constants for the second-order closure model for* A_u*=2.2,* A_v*=2.0, and* A_w*=1.4.*

Wilson and Shaw (1977)	*Value*
a_1	*0.30*
a_2	*1.58*
a_3	*20.8*
α	*0.07*
C	*0.12*
C_d	*0.20*

REFERENCES

Aylor, D., and J. Parlange. 1975. Ventilation required to entrain small particles from leaves. Plant Physiology **56**:97-99.

Aylor, D. E., and T. K. Flesch. 2001. Estimating spore release rates using a Lagrangian stochastic simulation model. Journal of Applied Meteorology **40**:1196-1208.

Aylor, D. E., N. P. Schultes, and E. J. Shields. 2003. An aerobiological framework for assessing cross-pollination in maize. Agricultural and Forest Meteorology **119**:111-129.

Ayotte, K. W., J. J. Finnigan, and M. R. Raupach. 1999. A second-order closure for neutrally stratified vegetative canopy flows. Boundary-Layer Meteorology **90**:189-216.

Baldocchi, D., E. Falge, L. H. Gu, R. Olson, D. Hollinger, S. Running, P. Anthoni, C. Bernhofer, K. Davis, R. Evans, J. Fuentes, A. Goldstein, G. Katul, B. Law, X. H. Lee, Y. Malhi, T. Meyers, W. Munger, W. Oechel, K. T. P. U, K. Pilegaard, H. P. Schmid, R. Valentini, S. Verma, T. Vesala, K. Wilson, and S. Wofsy. 2001. FLUXNET: A new tool to study the temporal and spatial variability of ecosystem-scale carbon dioxide, water vapor, and energy flux densities. Bulletin of the American Meteorological Society **82**:2415-2434.

Bessey, C. 1883. Remarkable fall of pine pollen. American Naturalists **17**:658.

Boyer, W.D. 1978. Heat accumulation: An easy way to anticipate the flowering of southern pines. Journal of Forestry **76**: 20-23

Bullock, J. M., and R. T. Clarke. 2000. Long distance seed dispersal by wind: measuring and modelling the tail of the curve. Oecologia **124**:506-521.

Cain, M. L., R. Nathan, and S. A. Levin. 2003. Long-distance dispersal. Ecology **84**:1943-1944.

Christey, M., and D. Woodfield. 2001. Coexistence of genetically modified and non-genetically modified crops. 427, Crop & Food Research Confidential Report, Riverdale, MD.

De Haan, P., and M. W. Rotach. 1998. A novel approach to atmospheric dispersion modelling: The Puff-Particle Model. Quarterly Journal of the Royal Meteorological Society **124**:2771-2792.

Di-Giovanni, F., P. Kevan, and J. Arnold. 1996. Lower planetary boundary layer profiles of atmospheric conifer pollen above a seed orchard in northern Ontario, Canada. Forest Ecology and Management **83**:87-97.

Di-Giovanni, F., P. K. PG, and M. Nasr. 1995. Settling velocities of some pollen and spores and their variability. Grana **34**:39-44.

Erdtman, G. 1937. Pollen grains recovered from the atmosphere over the Atlantic. Medd. Göteborgs Bot. Trädg **12**.

Fenning, T. M., and J. Gershenzon. 2002. Where will the wood come from? Plantation forests and the role of biotechnology. Trends in Biotechnology **20**:291-296.

Finnigan, J. 2000. Turbulence in plant canopies. Annual Review of Fluid Mechanics **32**:519-571.

Gura, T. 2001. The battlefields of Britain. Nature **412**: 760-763

Hails, R.S. 2000. Genetically modified plants - the debate continues. Trends Ecol. Evol. **15**: 14-18.

Hengeveld, R. 1989.*Dynamics of biological invasions*. Chapman and Hall, London. 160 p.

Higgins, S. I., J. S. Clark, R. Nathan, T. Hovestadt, F. Schurr, J. M. V. Fragoso, M. R. Aguiar, E. Ribbens, and S. Lavorel. 2003. Forecasting plant migration rates: managing uncertainty for risk assessment. Journal of Ecology **91**:341-347.

Hsieh, C. I., G. Katul, and T. Chi. 2000. An approximate analytical model for footprint estimation of scaler fluxes in thermally stratified atmospheric flows. Advances in Water Resources **23**:765-772.

Jarosz, N., B. Loubet, B. Durand, A. McCartney, X. Foueillassar, and L. Huber. 2003. Field measurements of airborne concentration and deposition rate of maize pollen. Agricultural and Forest Meteorology **119**:37-51.

Katul, G., B. Vidakovic, and J. Albertson. 2001. Estimating global and local scaling exponents in turbulent flows using discrete wavelet transformations. Physics of Fluids **13**:241-250.

Katul, G. G., and J. D. Albertson. 1998. An investigation of higher-order closure models for a forested canopy. Boundary-Layer Meteorology **89**:47-74.

Katul, G. G., and W. H. Chang. 1999. Principal length scales in second-order closure models for canopy turbulence. Journal of Applied Meteorology **38**:1631-1643.

Katul, G. G., C. D. Geron, C. I. Hsieh, B. Vidakovic, and A. B. Guenther. 1998. Active turbulence and scalar transport near the forest- atmosphere interface. Journal of Applied Meteorology **37**:1533-1546.

Katul, G. G., L. Mahrt, D. Poggi, and C. Sanz. 2004. One and two equation models for canopy turbulence. Boundary-Layer Meteorology **113**: 81-109.

Lanner, R. 1966. Needed: a new approach to the study of pollen dispersion. Silvae Genetica **15**.

Linacre, N., and P. Ades. 2004. Estimating isolation distances for genetically modified trees in plantation forestry. Ecological Modelling **179**: 247-257

Loos, C., R. Seppelt, S. Meier-Bethke, J. Schiemann, and O. Richter. 2003. Spatially explicit modelling of transgenic maize pollen dispersal and cross-pollination. Journal of Theoretical Biology **225**:241-255.

Mann, C., and M.L. Plumer. 2002. Forest biotech edges out of the lab. Science 295: 1626-1629.

Massman, W. J., and J. C. Weil. 1999. An analytical one-dimensional second-order closure model of turbulence statistics and the Lagrangian time scale within and above plant canopies of arbitrary structure. Boundary-Layer Meteorology **91**:81-107.

Messeguer, J. 2003. Gene flow assessment in transgenic plants. Plant Cell , Tissue and Organ Culture . **73**:201–212.

Moyes, C. L., J. M. Lilley, C. A. Casais, S. G. Cole, P. D. Haeger, and P. J. Dale. 2002. Barriers to gene flow from oilseed rape (Brassica napus) into populations of Sinapis arvensis. Molecular Ecology **11**:103-112.

Nathan, R., G. G. Katul, H. S. Horn, S. M. Thomas, R. Oren, R. Avissar, S. W. Pacala, and S. A. Levin. 2002. Mechanisms of long-distance dispersal of seeds by wind. Nature **418**:409-413.

Nathan, R., G. Perry, J. T. Cronin, A. E. Strand, and M. L. Cain. 2003. Methods for estimating long-distance dispersal. Oikos **103**:261-273.

Nichols, R., and G. Hewitt. 1994. The genetic consequences of long-distance dispersal during colonization. Heredity **72**:312-317.

OGTR, 2001. Risk analysis framework for license applications to the office of the gene technology regulator. Office of the Gene Technology Regulator, Canberra, Australia.

Okubo, A., and S. A. Levin. 1989. A Theoretical Framework for Data-Analysis of Wind Dispersal of Seeds and Pollen. Ecology **70**:329-338.

Oren, R., D. S. Ellsworth, K. H. Johnsen, N. Phillips, B. E. Ewers, C. Maier, K. V. R. Schafer, H. McCarthy, G. Hendrey, S. G. McNulty, and G. G. Katul. 2001. Soil fertility limits carbon sequestration by forest ecosystems in a CO2-enriched atmosphere. Nature **411**:469-472.

Parker, S., and T. Blush. 1996. Quantifying pollen production of loblolly pine (Pinus taeda L.) seed orchard clones. 163, Westvaco Forest Research Report.

Phillips, N., A. Nagchaudhuri, R. Oren, and G. Katul. 1997. Time constant for water transport in loblolly pine trees estimated from time series of evaporative demand and stem sapflow. Trees-Structure and Function **11**:412-419.

Poggi, D., J. D. Albertson, and G. G. Katul. 2005. Scalar dispersion within a model canopy: Measurements and Lagrangian models. Advances in Water Resources, **In press.**

Poggi, D., A. Porporato, L. Ridolfi, J. Albertson, and G. Katul. 2004a. The effect of vegetation density on canopy sublayer turbulence. Boundary-Layer Meteorology **111**: 565-587.

Poggi, D., G. G. Katul, and J. D. Albertson. 2004b. Momentum transfer and turbulent kinetic energy budgets within a dense model canopy. Boundary Layer Meteorology **111**:589–614.

Poggi, D., J. D. Albertson, and G. G. Katul. 2004c. A note on the contribution of dispersive fluxes to momentum transfer within canopies. Boundary Layer Meteorology **111**: 615-621.

Pope, S. B. 2000. Turbulent flows. Cambridge University Press, Cambridge.

Press, W., S. Teukolsky, W. Vetterling, and B. Flannery. 1992. Numerical Recipes in Fortran: The Art of Scientific Computing. Cambridge University Press, Cambridge.

Raupach, M. R. 1983. Near-Field Dispersion from Instantaneous Sources in the Surface-Layer. Boundary-Layer Meteorology **27**:105-113.

Raupach, M. R. 1987. A Lagrangian Analysis of Scalar Transfer in Vegetation Canopies. Quarterly Journal of the Royal Meteorological Society **113**:107-120.

Raupach, M. R. 1989a. Applying Lagrangian Fluid-Mechanics to Infer Scalar Source Distributions from Concentration Profiles in Plant Canopies. Agricultural and Forest Meteorology **47**:85-108.

Raupach, M. R. 1989b. A practical lagrangian method for relating scalar concentrations to source distributions in vegetation canopies. Quarterly Journal of the Royal Meteorological Society **115**:609--632.

Raupach, M. R. 1989c. A Practical Lagrangian Method for Relating Scalar Concentrations to Source Distributions in Vegetation Canopies. Quarterly Journal of the Royal Meteorological Society **115**:609-632.

Raupach, M. R., J. J. Finnigan, and Y. Brunet. 1996. Coherent eddies and turbulence in vegetation canopies: The mixing-layer analogy. Boundary-Layer Meteorology **78**:351-382.

Raupach, M. R., and R. H. Shaw. 1982. Averaging Procedures for Flow within Vegetation Canopies. Boundary-Layer Meteorology **22**:79-90.

Reynolds, A. M. 1998a. Comments on the 'Universality of the Lagrangian velocity structure function constant (C-0) across different kinds of turbulence'. Boundary-Layer Meteorology **89**:161-170.

Reynolds, A. M. 1998b. A Lagrangian stochastic model for the trajectories of particle pairs and its application to the prediction of concentration variance within plant canopies. Boundary-Layer Meteorology **88**:467-478.

Reynolds, A. M. 1998c. Modelling particle dispersion within a ventilated airspace. Fluid Dynamics Research **22**:139-152.

Reynolds, A. M. 1998d. On the formulation of Lagrangian stochastic models of scalar dispersion within plant canopies. Boundary-Layer Meteorology **86**:333-344.

Reynolds, A. M. 2000. On the formulation of Lagrangian stochastic models for heavy-particle trajectories. Journal of Colloid and Interface Science **232**:260-268.

Reynolds, A. M., and J. E. Cohen. 2002. Stochastic simulation of heavy-particle trajectories in turbulent flows. Physics of Fluids **14**:342-351.

Rieger, M. A., M. Lamond, C. Preston, S. B. Powles, and R. T. Roush. 2002. Pollen-mediated movement of herbicide resistance between commercial canola fields. Science **296**:2386-2388.

Righter, F., and J. Duffield. 1951. A summary of interspecific crosses in the genus Pinus made at the Institute of Forest Genetics. J. Hered. **42**:75-80.

Rodean, H. 1996. Stochastic Lagrangian Models of Turbulent Diffusion. American Meteorological Society, Boston, 83 pages.

Sawford, B. L., and F. M. Guest. 1991. Lagrangian Statistical Simulation of the Turbulent Motion of Heavy-Particles. Boundary-Layer Meteorology **54**:147-166.

Siqueira, M., and G. Katul. 2002. Estimating heat sources and fluxes in thermally stratified canopy flows using higher-order closure models. Boundary-Layer Meteorology **103**:125-142.

Siqueira, M., G. Katul, and C. T. Lai. 2002. Quantifying net ecosystem exchange by multilevel ecophysiological and turbulent transport models. Advances in Water Resources **25**:1357-1366.

Siqueira, M., C. T. Lai, and G. Katul. 2000. Estimating scalar sources, sinks, and fluxes in a forest canopy using Lagrangian, Eulerian, and hybrid inverse models. Journal of Geophysical Research-Atmospheres **105**:29475-29488.

Smouse, P. E., R. J. Dyer, R. D. Westfall, and V. L. Sork. 2001. Two-generation analysis of pollen flow across a landscape. I. Male gamete heterogeneity among females. Evolution **55**:260-271.

Stockmarr, A. 2002. The distribution of particles in the plane dispersed by a simple 3-dimensional diffusion process. Journal of Mathematical Biology **45**:461-469.

Strauss, S., W. H. Rottman, A. Brunner, L.A. Sheppard. 1995. Genetic engineering of reproductive sterility in forest trees. Molecular Breeding **1**: 5-26.

Strauss, S., M.M. Campbell, S. N. Pryor, P. Coventry, and J. Burley. 2001. Plantation Certification and Genetic Engineering: Ban on Research is Counter Productive. Journal of Forestry - December: 4-7.

Thomson, D. J. 1987. Criteria for the selection of stochastic-models of particle trajectories in turbulent flows. Journal of Fluid Mechanics **180**:529--556.

Tuskan, G., T. Tschaplinski, B. Franc, and N. Edwards. 1992. UV-B radiation reduces germination capacity of loblolly pine and red spruce pollen. *in* In Proc. 12th North American Forest Biology Workshop. Ontario Ministry of Natural Resources, Sault Ste. Marie, Ontario.

Wilson, J. 1988. A Second Order Closure Model for Flow through Vegetation. Boundary-Layer Meteorology **42**:371–392.

Wilson, J. D., and B. L. Sawford. 1996. Review of Lagrangian stochastic models for trajectories in the turbulent atmosphere. Boundary-Layer Meteorology **78**:191-210.

Wilson, N., and R. Shaw. 1977. A Higher Order Closure Model for Canopy Flow. Journal of Applied Meteorology **16**:1198–1205.